Errors in model development; the verification of a thermo-hygro-corrosive model for radioactive waste storage applications

Christopher Nahed, Jacques de Lamare, Antoine Pasteau

CSMA 2024
16ème Colloque National en Calcul des Structures
13-17 Mai 2024, Presqu'île de Giens (Var)

Errors in model development; the verification of a thermo-hygro-corrosive model for radioactive waste storage applications

C. Nahed[1], J. de Lamare[2], A. Pasteau[3]

[1] *Service d'études Mécaniques et Thermiques, Université Paris-Saclay, CEA, christopher.nahed@cea.fr*
[2] *Service de La Corrosion et Du Comportement des Matériaux Dans Leur Environnement, Université Paris-Saclay, CEA, jacques.de-lamare@cea.fr*
[3] *Andra, R&D Division, 1/7 Rue Jean Monnet, 92298, Châtenay-Malabry, France, antoine.pasteau@andra.fr*

Résumé — Mathematical errors are omnipresent in physics and engineering. In fact, errors are unavoidable when conducting experiments, modelling physical phenomena and when solving theoretical models either by hand or on digital computers. The ubiquity of errors in accuracy and precision makes their quantification and control fundamental. The standardised definitions of modelling accuracy and calculation precision are discussed; and an analysis of calculation precision control is presented for a numerical implementation of a multiphysics model used for a radioactive waste storage application.
Mots clés — radioactive waste storage structure, model verification, multiphysics modelling, method of manufactured solutions.

1 Introduction and context

Modelling and simulation of multiphysics problems is essential for many applications in engineering. The mathematical modelling of a physical system is developed on diverse hypotheses that limit the redundancies of the infinite number of mathematical terms that can be used in an equation. The hypotheses, if chosen and modelled correctly, minimize the accuracy error δa of the model which ensures sufficient physical representativity of the mathematical model. An accurate mathematical model serves scientists as a mathematical tool with which simulations can be performed for use in their theoretical studies. Moreover, because simulation results depend on a variety of numerical parameters (discretisation size, convergence criteria, scheme type etc...) a precision error δp associated with the calculated theoretical response is generated. These errors that are thus associated to any model and calculation are scientifically inherent and can never be totally omitted. However, the quantification and control of δa and δp is fundamental to a scientific study because it permits scientists to design their applications in accordance with the quantified errors.

1.1 Verification and validation of numerical models

The verification and validation of numerical models is simply the quantification and control of the precision error δp and the accuracy error δa. Moreover, the verification of a numerical model is a purely mathematical effort that is based on the quantification and control of δp by studying its sensitivity to the main numerical parameters of the computational model. As for the validation of said model, it manifests as both a mathematics and physics exercise where δa, which describes the error between the results of a verified model and the real response, is minimised by improving the physical representativity of the model. These definitions are based on the standardised descriptions of the *Qualification des outils de calcul scientifique utilisés dans la démonstration de sûreté nucléaire* published by French Nuclear Safety Authority, and the standard for verification and validation published by the American Society of Mechanical Engineers [1, 2]. The numerical distinction between δp and δa is schematised in figure 1 where δp is represented as a precision error bar while δa is schematised as the numerical distance between some real response and the theoretical response issue from the simulation of the model.

Referring to the schematic in figure 1, it is clear that the numerical scientist seeks to ensure that the total sum of his errors is less than the experimental error (schematised as δe). This ensures that

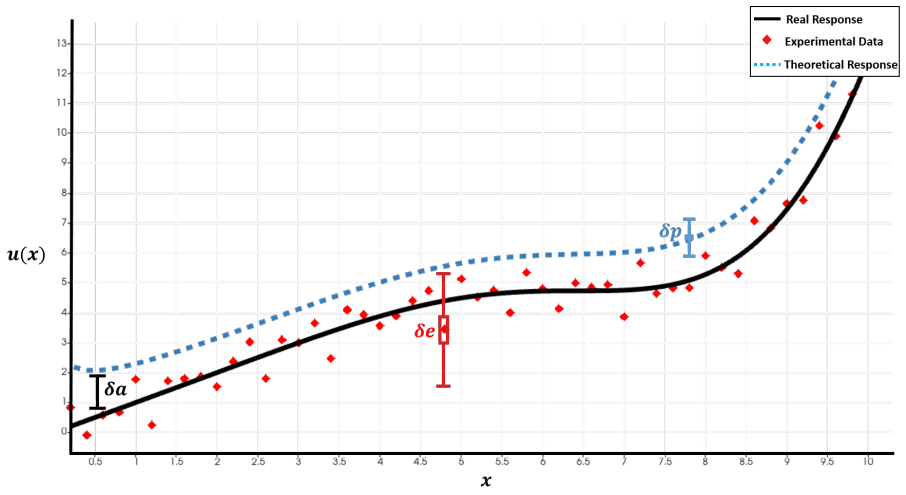

FIGURE 1 – Schematic of δe, δa and δp that represent experimental, accuracy (or modelling) and precision (or simulation) errors, respectively. For illustration purposes only.

the theoretical response issue from the numerical simulation of the mathematical model is within the sensitivity range of the reference experiment. This can be expressed as :

$$\delta a + \delta p \lesssim \delta e$$

where the above approximate inequality implies the need to quantify and control both δp and δa. A loose definition of error quantification and control is the numerical approximation and the comprehension of their behaviours and sensitivities (w.r.t the plethora of model and numerical parameters), respectively. Following the standard definitions from [1, 2] the quantification and control of δp is considered as numerical simulation tool verification, while the minimisation of $\delta a + \delta p$ is considered as model validation.

The rest of the discussion in this work is centered around a verification study performed on a multiphysics model our group developed in [3]. For a detailed mathematical analysis of the multitude of accuracy error sources and model validation, the interested reader is referred to chapter 5 in [2].

1.2 Motivating our multiphysics model: the French radioactive waste storage application

The *Agence Nationale pour la Gestion des Déchets Radioactifs* (ANDRA) is the French national agency for the management of radioactive waste and it mainly offers its services to the French government. The ANDRA is currently designing and will construct the *Centre Industriel de Stockage Géologique* (CIGEO) for the reversible (and eventually permanent) storage of medium and high activity radioactive waste [4, 5]. The ANDRA along with its collaborators at the *Commissariat à l'Energie Atomique et aux Energies Alternatices* (CEA) have invested in the development of a thermo-hygro-corrosive model of the storage tunnels (named alveoli by ANDRA) [3]. The main purpose behind the model is to approximate corrosion rates and rust accumulation along the steel walls of the many alveoli to be built in their underground waste storage site [5, 3]. Figure 2 illustrates the gallery and perpendicularly branching alveoli which are designed to store the waste packages. With the primary construction material of the alveoli being steel, and by being exposed to a humid geological environment, to the waste heat from the radioactive waste and to air, the accumulation of rust is an important variable to approximate over time [3]. Thus, this motivates the numerical implementation of the multiphysics model as it is described in [6].

2 Physical and numerical model

The physics behind the model is based on the dominant phenomena identified by de Lamare in the various technical reports found in [3]. The model physics is described using non-linear partial differential equations (PDE) that mathematically describe heat and water vapour transport as well as condensation

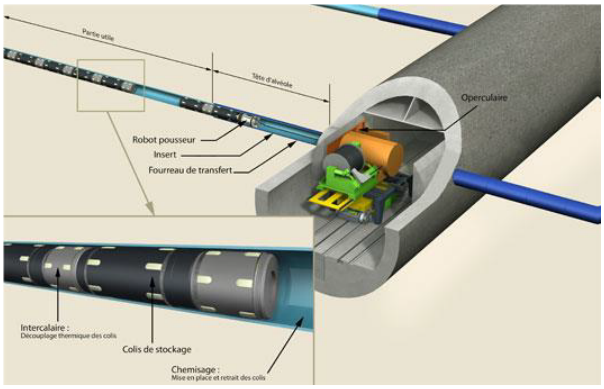

FIGURE 2 – Illustration of the CIGEO radioactive waste storage gallery and *alveoli* [5]

and evaporation, oxygen transport and its reduction, and the corrosion of steel. As for the numerical implementation of the physical model, it is based on Nahed's work in [6] where a Crank-Nicolson temporal scheme pilots the time stepping algorithm, while a Newton-like residual minimisation scheme ensures calculation convergence at every time step. The numerical implementation is performed on the Cast3M finite element toolbox [7]. Figure 3 illustrates a simplified geometry used in the testing of the numerical implementation of the physical model. Note that the geometric arguments that follow are based on the geometric details schematised in figure 3.

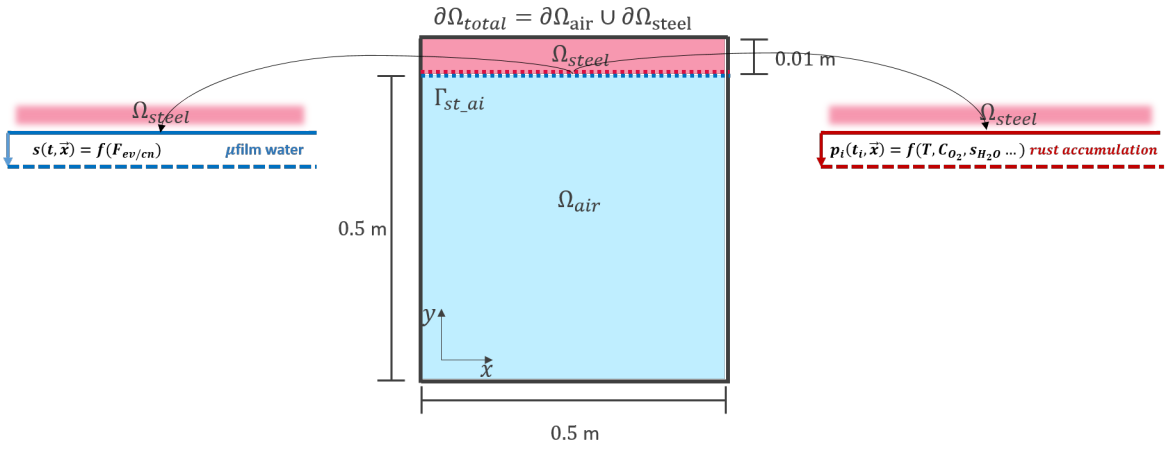

FIGURE 3 – Schematic of the reference geometry used in a first implementation of the model [3].

2.1 Physical model

A brief description of the physical model is presented here, and the interested reader is referred to [3] for details [1].

2.1.1 Heat transfer

Volume phenomena

The heat transfer in the steel Ω_{steel} and air Ω_{air} domains are modelled using the following PDE [3] :

$$\rho c_p \frac{\partial T}{\partial t} = \nabla \cdot (\lambda \nabla T) \tag{1}$$

where ρ, c_p and λ are the mass density, specific heat and thermal conductivity. These coefficients are functions of domain Ω, temperature T and humidity C_{H_2O}. The thermal coefficients are defined by the

1. Access to the technical reports is not guaranteed by the author.

following piece-wise function :

$$(\rho, c_p, \lambda)_\Omega = \begin{cases} f(T) & \boldsymbol{x} \in \Omega_{steel} \\ f(T, C_{H_2O}) & \boldsymbol{x} \in \Omega_{air} \end{cases} \tag{2}$$

Interfacial phenomena

The heat transfer that occurs across the steel-air interface Γ_{st-ai} is modelled by a thermal discontinuity constraint and by an evaporation/condensation flux [3]. The equation that represents thermal discontinuity is :

$$h_{ex}(T_{\Gamma_{steel}} - T_{\Gamma_{air}}) = (\lambda \nabla T)_{\Gamma_{air}} \cdot \boldsymbol{n} \tag{3}$$

where h_{ex} is a convection coefficient and $\boldsymbol{n}$ the normal unit vector at the interface. The equation that models the evaporation/condensation flux is the following :

$$\big((\lambda \nabla T)_{\Gamma_{steel}} - (\lambda \nabla T)_{\Gamma_{air}}\big) \cdot \boldsymbol{n} = (L_v \cdot M_{H_2O})\, F_{ev/cn} \tag{4}$$

where L_v is the latent heat of evaporation, M_{H_2O} the molar mass of water and $F_{ev/cn}$ the evaporation/condensation flux. The flux $F_{ev/cn}$ is modelled by the following equation [3] :

$$F_{ev/cn} = -D_{H_2O}\, \kappa \Big(C_{H_2O\Gamma_{air}} - C_{sat,\Gamma_{acier}} \big(\frac{T_{acier}}{T_{air}}\big)^{1/2} \Big)\, \exp^{(D\kappa^2\, t)} \exp^{(\kappa^2\, (Dt)^{1/2})} \tag{5}$$

where D_{H_2O} is the diffusivity of vapor, C_{sat} the saturating concentration of water vapour (see equation (12), section 2.1.2) and $\kappa = f(T_{\Gamma_{air}})$.

2.1.2 Vapour Transfer

Volume and surface phenomena

Vapour transfer in the air domain Ω_{air} along with its boundary condition on Γ_{air} is modelled by the following PDEs [3] :

$$\frac{\partial C_{H_2O}}{\partial t} = \nabla \cdot (D_{H_2O} \nabla C_{H_2O}) \tag{6}$$

$$-D_{H_2O}\, (\nabla C_{H_2O}) \cdot \boldsymbol{n} = F_{ev/cn} \qquad \text{on} \quad \Gamma_{air} \tag{7}$$

where the diffusivity D_{H_2O} is a function of temperature, defined as :

$$D_{H_2O} = f(T) \qquad \boldsymbol{x} \in \Omega_{air} \tag{8}$$

The vapour transfer occurs across a thin film of water (μfilm) that is simply modelled as a source/sink positioned atop the steel surface Γ_{steel}. Since both the dynamic and kinematic effects of the μfilm are negligible at the scale of the *alvéole*, the μfilm is uniquely modelled by a mass conservation equation. This implies that tracking the interface in time is unnecessary ; therefore, the μfilm is not geometrically included nor numerically meshed [3, 6]. Referring to figure 3 where we note the representation of the μfilm as a simple source/sink for the vapor transfer boundary condition of equation (7). The water film also serves as the environment where oxygen reduction occurs (details in the following subsections). The rate of growth/decrease of the μfilm depends on humidity conditions of the neighbouring air and is also a function of the evaporation/condensation flux as defined in (5). The growth/decrease rate of the μfilm is defined as :

$$\frac{ds(\boldsymbol{x}_\Gamma, t)}{dt} = \Big(\frac{M_{H_2O}}{\rho_{H_2O}}\Big) F_{ev/cn}(\boldsymbol{x}_\Gamma, t) \qquad \boldsymbol{x}_\Gamma \in \Gamma_{steel} \tag{9}$$

where $s(\boldsymbol{x}_\Gamma, t)$ is the film height that could vary across steel surface Γ_{steel}. Regardless of the simple μfilm model, it strongly interacts with the temperature and concentration variables *via* the following humidity conditions :

$$\textbf{IF}, \text{ a } \mu\text{film exists, } s(\boldsymbol{x}_\Gamma, t) > 0 :$$

$$F_{ev/cn} = \text{equation (5)} \tag{10}$$

$$
\begin{aligned}
\textbf{ELSE}, \quad s(\boldsymbol{x}_\Gamma, t) &= 0 : \\
\textbf{IF}, \quad & T(\boldsymbol{x}_{\Gamma_{steel}}, t) < T_{dew}(\boldsymbol{x}_{\Gamma_{air}}, t) : \\
& F_{ev/cn} = \text{equation (5)} \\
\textbf{ELSE}, & \\
& F_{ev/cn} = 0
\end{aligned}
$$

where T_{dew} is the dew point temperature of air defined by the Rankine equation [3] :

$$T_{dew} = \frac{5120}{13.7 - \ln\left(\frac{R\, C_{H_20} T_{air}}{101.325 \times 10^3}\right)} \tag{11}$$

where R is the universal gas constant. The saturating vapour concentration C_{sat} is :

$$C_{sat} = \frac{101.325 \times 10^3}{R\, T_{steel}} \exp\left(13.7 - \frac{5120}{T_{steel}}\right) \tag{12}$$

2.1.3 Oxygen Transfer

Volume and surface phenomena

Oxygen transfer in the air domain Ω_{air} along with its boundary condition on Γ_{air} is modelled by the following PDEs [3] :

$$\frac{\partial C_{O_2}}{\partial t} = \nabla \cdot (D_{O_2} \nabla C_{O_2}) \tag{13}$$

$$-D_{O_2}(\nabla C_{O_2}) \cdot \boldsymbol{n} = \Phi(C_O, D_O) \qquad \text{on} \quad \Gamma_{air} \tag{14}$$

where Φ is the oxygen consumption rate, the diffusivity D_{O_2} is a function of temperature, defined as :

$$D_{O_2} = f(T) \qquad \boldsymbol{x} \in \Omega_{air} \tag{15}$$

furthermore, the oxygen transfer at the Γ_{air} surface is modelled by a reduction equation where oxygen is consumed by the corrosion reaction. The conditions on the reduction reaction are the following :

$$
\begin{gathered}
\textbf{IF}, \text{ a } \mu\text{film exists}, s(\boldsymbol{x}_\Gamma, t) > 0 : \\
\Phi = C_O\, D_{O(T_{\Gamma_{steel}})} \frac{(1 - \exp(-(L_0 - l)/\lambda_r))}{(d + (\tau/\varepsilon)(l + \lambda_r))} \qquad (16) \\
\text{for} \qquad C_O = H \frac{C_{O_2}}{R\, T_{\Gamma_{air}}} \quad \text{where H is Henry's constant} \\
\textbf{ELSE}, \ s(\boldsymbol{x}_\Gamma, t) = 0 : \\
\Phi = 0
\end{gathered}
$$

where the various corrosion rate parameters (L_0, l, λ_r, d, τ, ε) and variables in equation (16) are detailed in [3].

2.1.4 Damage by corrosion

Before presenting the quantitative model (as developed in [3]) that describes damage by corrosion, we remind the reader of the reduction-oxidation (redox) reaction that occurs along oxygen-iron interaction zones :

$$\mathrm{Fe} \longrightarrow \mathrm{Fe}^{2+} + 2e^- \tag{17}$$

$$\frac{1}{2}\mathrm{O}_2 + 2e^- + \mathrm{H}_2\mathrm{O} \longrightarrow 2\mathrm{OH}^- \tag{18}$$

$$\gamma - \mathrm{FeOOH} + \mathrm{H}^+ + e^- \longrightarrow \gamma - \mathrm{FeOHOH} \tag{19}$$

where $\gamma-$FeOOH represents the lepidocrocite type rust, which makes up the majority of the rust layer in our model [3]. The corrosion model considers a relative time based on the wet time of the steel surface. That is, there is a wet cycle i that triggers the corrosion damage phenomena. This implies that if the steel surface is dry, the relative time nullifies $t_i = 0$ and the total corrosion damage p_i stops until further wetting. The model is schematised in figure 3 and is summarised in the following :

$$
\begin{aligned}
\textbf{IF,} \quad & \text{a } \mu\text{film created on dry } d\Gamma_{steel},\ s(\boldsymbol{x}, t_i = 0) = 0 \quad \& \quad \delta s(\boldsymbol{x}, t_i = 0) = \frac{ds}{dt}\delta t > 0 : \\
t_i &= [0,\ t_{dry}] \qquad \text{where } t_{dry} \text{ is the relative time for the element that dries} \\
p_i &= p_i{}' + p_i{}'' \\
\text{for} \quad p_i{}' &= 0.5\,\beta\, n\, e\, S_a (1-\varepsilon)(V_{mFe}/V_{mFeOOH})(p_{i-1} - l)\frac{t_i}{t_{Fi}} \\
\text{for} \quad p_i{}'' &\propto \Phi \cdot t_i
\end{aligned}
$$

$$
\begin{aligned}
\textbf{ELSE}, \ : \\
&\textbf{IF}, \quad s(\boldsymbol{x}_{\Gamma_{steel}}, t) > 0 \quad \& \quad t_i > 0 : \\
&\qquad \text{IDEM, see IF condition above} \\
&\textbf{IF}, \quad s(\boldsymbol{x}_{\Gamma_{steel}}, t) = 0 \quad \& \quad t_i = 0 : \\
&\qquad p_i = 0
\end{aligned}
$$

where $p_i{}'$ is the lepidocrocite reduction damage variable (associated to reactions (17) and (19)) and $p_i{}''$ the iron redox damage variable (associated to reactions (17) and (18)). For the rest of the details about the various parameters and variables, see [3].

Note that in the verification study, the outer boundaries of the domain $\partial\Omega_{total}$ are considered adiabatic and impermeable. This choice simplifies the analysis performed in the study. Furthermore, we note that the data used for the thermophysical properties in the above equation are compiled in de Lamare's works [3].

2.2 Numerical model

With the details behind the numerical model out of the scope of this text (see [6] for details), a description and schematic of the multiphysics algorithm are presented. The physical model is partitioned into four numerical modules where the modules communicate with the other modules they are coupled to. Depending on the coupling strength [2] between the modules, the linearisation method and coupling scheme slightly varies. The schematic in figure 4 illustrates the multiphysics algorithm used as based on [6].

3 Verification of the multiphysics model implementation

The verification of the thermo-hygro-corrosive model was preliminarily performed in [8] where the thermal and hygrometric modules were verified in an isolated and decoupled manner. The decoupled strategy allowed for the code verification of the multiple scripts of the computer program. In this extended abstract, we briefly present the method of manufactured solutions (MMS) as defined by [2]. The MMS is a simple yet powerful technique that allows the use of analytical solutions for the exact calculation of the precision error δp. Before discussing the MMS further, we first present the different components of the precision error δp :

$$\delta p = \delta p_h + \delta p_{iter} = u_{num} - u_M \tag{20}$$

where δp_h is the discretisation error, δp_{iter} the iteration error, u_{num} the numerical solution and u_M the manufactured and analytical solution. The δp_h is the error contribution stemming from spatial and temporal discretisations and is the error to quantify and control in a verification study ; whereas, δp_{iter} is the

2. The author is aware that this term is vague and hopes to clarify it in a future publication.

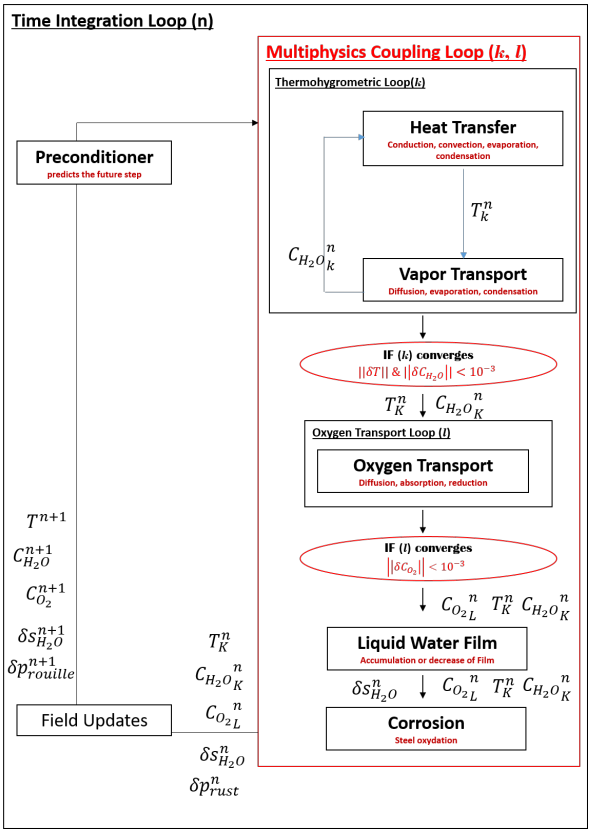

FIGURE 4 – Schematic of the multiphysics algorithm used to solve the physical model [6].

error contribution that is generated by iterative schemes that linearise non-linear systems. The δp_{iter}, if not controlled at every iteration of a calculation, will pollute the order of estimation of δp. Thus, a rule of thumb is to reduce the normalised value of δp_{iter} to be at least 0.1% of the δp_h so as to not bias a convergence analysis performed on δp [2]. For example and in our study, the reduction and control of δp_{iter} is ensured by the algorithm as is illustrated in figure 4 where the convergence conditions in the *Boucles multiphysique* k, l block can be tuned to any given value [6]. Theron, the difference $u_{num} - u_M$ is considered representative of $\delta p \approx \delta p_h$.

The analytical but manufactured solution u_M is designed to exercise all the numerically implemented terms of the system of PDEs of interest, and little care about the physical representativity of the solution is necessary as long as u_M respects the mentioned numerical requirement. The "manufacturing" of the solution u_M is based on the following concept, given the following system for an arbitrary set of differential operators $\mathcal{L}(u)$ and $\mathcal{B}(u)$:

$$\begin{cases} \mathcal{L}(u) = 0 & \forall \boldsymbol{x} \in \Omega, \\ \mathcal{B}(u) = 0 & \forall \boldsymbol{x} \in \partial\Omega \end{cases} \tag{21}$$

then, assume a closed form solution $u_M = f(\boldsymbol{x},t)$ sufficiently derivable and continuous that does not necessarily satisfy system (21). Inputting u_M in system (21) we get :

$$\begin{cases} \mathcal{L}(u_M) = g(\boldsymbol{x}_\Omega,t) \neq 0, \\ \mathcal{B}(u_M) = k(\boldsymbol{x}_{\partial\Omega},t) \neq 0 \end{cases} \longrightarrow \begin{cases} \mathcal{L}_\mathcal{M}(u_M) = 0 = \mathcal{L}(u_M) - g(\boldsymbol{x}_\Omega,t), \\ \mathcal{B}_\mathcal{M}(u_M) = 0 = \mathcal{B}(u_M) - k(\boldsymbol{x}_{\partial\Omega},t) \end{cases} \tag{22}$$

where $\mathcal{L}_\mathcal{M}(u_M)$ and $\mathcal{B}_\mathcal{M}(u_M)$ make the new system of equations that correspond to the manufactured solution u_M.

As shown in [8], simple yet sufficient manufactured solutions were compared to the output of both the thermal and vapor transfer modules. This study was essential for both code and scheme verification of the modules. Moreover, in an internal study (to be published in a future work) a *meta*-verification study that verifies the multiphysics scheme (see figure 4) is performed.

4 Conclusion

Since both modelling and simulation of multiphysics problems has become essential in modern day engineering, accurate physical models need to be implemented as precise numerical models. We present, *via* our radioactive waste storage application, a simple yet powerful verification methodology that allows for both the quantification and control of the precision errors associated with numerical implementations. Thus, although numerical errors (simulation precision errors) are ubiquitous in simulation engineering, they can be managed through implementation rigour and verification.

Références

[1] Autorité de Sécurité Nucléaire. Qualification des outils de calcul scientifique utilisés dans la démonstration de sûreté nucléaire—1re barrière. Technical report, Technical Report Autorité de Sécurité Nucléaire : Paris, France, 2017.

[2] American Society of Mechanical Engineers. *Standard for Verification and Validation in Computational Fluid Dynamics and Heat Transfer : An American National Standard*. American Society of Mechanical Engineers, 2009.

[3] J. de LAMARE. Modèlisation de la corrosion atmosphèrique : condensation de la vapeur d'eau contenue dans l'air ambiant - Synthèse de l'action CORRAT 2016 : modèle de corrosion atmosphérique en micro-tunnel HA - Bilan Action CORRAT 2017 - Modèle CORRAT étendu. Technical report, CEA, 2014 - 2016 - 2017 - 2020.

[4] Site de l'ANDRA. https ://www.andra.fr.

[5] Site gouvernementale de CIGEO. https ://www.cigeo.gouv.fr.

[6] Christopher Nahed. Implémentation numérique du Modèle Physique CORRAT, dans Cast3m. Technical report, 2022.

[7] Cast3m Web site. `http://www-cast3m.cea.fr/`.

[8] K. Cantenot. *Etude de vérification du modele thermo-hygrometrique d'une alveole de stockage souterrain de dechets radioactifs*. Manuscrit de thèse de master, Université Paris XIII, 2023.